Journal of Imaging Science and Technology® 66(3): 030507-1–030507-10, 2022.

Paper Temperature Prediction Modeling in Production Printing System by Using Machine Learning

Takamasa Hase
Ricoh Digital Products Business Unit, Ricoh Company, Ltd., 2-7-1 Izumi, Ebina, Kanagawa, 243-0460, Japan
E-mail: takamasa.hase@jp.ricoh.com

Shunsuke Kawasaki, Erdem Dursunkaya, and Takumi Ishikura
Department of Mechanical Engineering, Tokyo Institute of Technology, 2-12-1 Ookayama, Meguro, Tokyo, 152-8550, Japan

Kaori Hemmi
Ricoh Graphical Communications Business Unit, Ricoh Company, Ltd., 2-7-1 Izumi, Ebina, Kanagawa, 243-0460, Japan

Kimiharu Yamazaki
Advanced Technology R&D Division, 2-7-1 Izumi, Ebina, Kanagawa, 243-0460, Japan

Shinichi Kuramoto, Koichi Kato, and Kazuyoshi Fushinobu
Department of Mechanical Engineering, Tokyo Institute of Technology, 2-12-1 Ookayama, Meguro, Tokyo, 152-8550, Japan

Abstract. *In the production printing industry, printing speed of not only plain paper but also special paper has improved. After toner fixing process, when heat is applied to toner to fix it on paper, the toner on the paper stick to each other on outlet tray leading to toner blocking problem in high-speed printing. To control a paper cooling device, accurate prediction of the outlet paper temperature is useful. This, however, is not so easy; printing conditions and paper types are too diverse to conduct the experiments and the mechanism of the printer is also too complex to develop the physical model. The machine learning (ML) algorithm to predict the paper temperature was proposed under the limited printing conditions. In this research, the ML model that could improve prediction accuracy and generalization capability was developed by selecting appropriate paper properties for the input.* © *2022 Society for Imaging Science and Technology.*
[DOI: 10.2352/J.ImagingSci.Technol.2022.66.3.030507]

1. INTRODUCTION

There are several printing methods in the printing industry, which are broadly classified into printing with master and printing without master. The offset printing, which is a representative of the printing with master, is a printing method that has superior reproducibility for photographs and colors and is suitable for a large amount of printing that has a high definition image quality. However, it is not suitable for a small amount of printing because the master-making causes high cost. Also, the offset printer has a large scaled mechanism and it needs technical adjustment by the professional operator.

Received Feb. 21, 2021; accepted for publication Dec. 5, 2021; published online Jan. 20, 2022. Associate Editor: Nemanja Kasikovichase.
1062-3701/2022/66(3)/030507/10/$25.00

The advantages of the digital printing, which is a representative of the printing without master, are short delivery time, different contents for each sheet, and extremely small lots. Further, the electro-photographic printing method is capable of high-speed printing onto more paper types than the inkjet printing method, and there are various lineups ranging from office type to production printing type.

Especially in the production printing industry, the printing speed of not only plain paper but also special papers has been improved [1, 2]. Accordingly, it could not lower the paper temperature sufficiently on the transportation route in the large volume printing. It causes the toner blocking problem, when toner on the paper stick to each other when continuously printed paper is stacked.

To solve this problem, the cooling device has been developed [3]. It has a U-shaped conveying path and fans for cooling the paper. In designing the cooling device and controlling the temperature, accurate prediction of the outlet paper temperature would be useful.

In earlier studies, the physical model in the fuser process was developed [4]. The profile of the paper surface was measured and the contact area was also calculated by simulating deformation of the paper surface and the fuser surface. Among other previous studies, the effect of paper properties on the thermal interactions in the fusing nip was investigated [5], the measuring method of the thermal properties of paper has been proposed [6], and the chemical and physical properties of paper that affect fusing fix was characterized [7]. This, however, is not so easy; the mechanism of the printer and fusing process is typically complex. It is difficult to develop the physical model to represent the thermal interactions in the fusing nip and it is also difficult to measure the thermal properties of paper

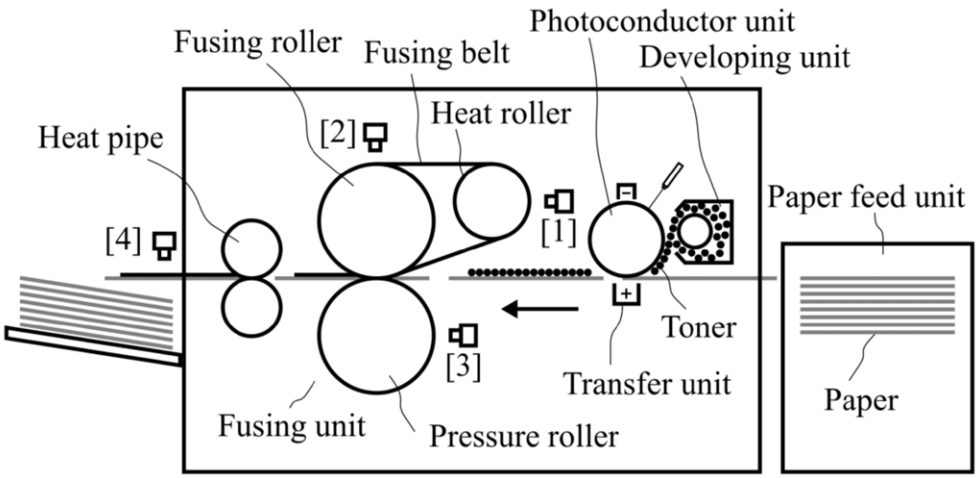

Figure 1. Experimental set-up.

accurately because paper is composed of fibers, moisture, surface coating layer and smoothness of paper surface varies by paper type. Physical models are based on governing equations, and the degrees of freedom a model can take are relatively limited. If the model cannot represent the experimental results, the cause requires investigation and correction. If the mechanism is complex, it is difficult to reproduce the experimental results.

This work proposes using ML as an alternative to estimate the outlet paper temperature in the production printing system. ML is a set of algorithms that build a model based on the training data in order to make predictions without any human help and has numerous parameters, which allows for a high degree of freedom. On exposure to sufficient data, ML algorithms can find relations between the input and the output and estimate the output of data based on conditions. It is being extensively used in various fields, most prominently in computer vision, spam filtering, driverless cars [8]. It has also found a niche in engineering, particularly material property prediction and thermal-fluid modelling [9]. In the printing industry, AI technology is used to minimize printing failures [10].

The ML algorithm using Artificial neural network (ANN) to estimate the outlet paper temperature was proposed [11, 12]. Although there was a correlation between the predicted value and the measured value under the limited training conditions, it was not validated under other paper types and other printing modes. Recently, by applying appropriate preprocessing to the data and selecting the appropriate inputs, accurate prediction under various conditions is obtained [13]. However, it has not been verified which input is effective for highly accurate prediction of paper temperature.

The purpose of this work is not only to obtain a highly accurate prediction model under various conditions, but also to verify how to select the physical properties of paper as the input to improve the prediction accuracy by using the ML algorithms.

2. EXPERIMENTAL SET-UP

2.1 *Overview of Production Printing System*

Experiments were performed by using the production printing system of the electro-photographic method that can print 80 sheets in A4 size per minute. This system consists of paper feed unit, developing unit, photoconductor unit, transfer unit, fusing unit and heat pipe.

The electro-photographic image forming process is a process of forming the image of electro-static charge on a photoconductor, attaching the charged toner to the photoconductor by using electro-static force, and transferring and fixing the toner on paper. The heat pipe lowers the paper temperature, and blowing air also lowers the heat pipe temperature. Figure 1 shows the configuration of experimental set-up used in this study and the electro-photographic image forming process.

2.2 *Temperature Sensors*

There are 4 sensors used for this experiment, as shown in Fig. 1 and Table I. Sensor [1] is for the heat roller temperature, Sensor [2] is for the fusing roller temperature and Sensor [3] is for the pressure roller temperature. The type of these sensors is the radiation thermometer. Sensor [2] can also measure its own temperature, which is used to compensate the detected temperature with the temperature of the sensor itself. This temperature has a correlation with the ambient temperature at the sensor location. Sensors [1]–[3] were originally installed in the mass production machine to control the fusing temperature. Sensor [4] is the radiation thermometer for measuring the outlet paper temperature. Sensor [4] were installed only for this experiment.

2.3 *Temperature Control of Fixing Process*

The fixing process is the process of applying heat and pressure to the toner and the paper, melting the toner and sticking it to the paper.

The heat for the fixing process is applied to the fusing belt from the heat roller, and the fusing belt rotates and moves

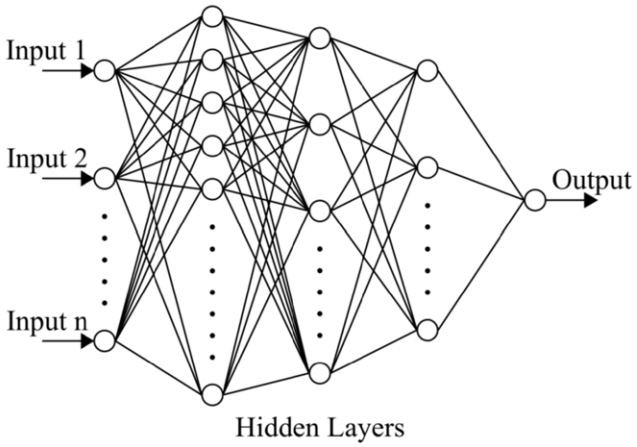

Figure 2. Schematic of ANN.

Table I. Temperature sensors

Sensor No. in Fig. 1	Target	Sensor type
[1]	Heat roller	Radiation thermometer
[2]	Fusing roller	Radiation thermometer
[2]	Fusing roller sensor	Radiation thermometer
[3]	Pressure roller	Radiation thermometer
[4]	Outlet paper	Radiation thermometer

to the nip portion between the fusing roller and the pressure roller. The fusing temperature is controlled by the heat roller and the temperature sensor [1] in Fig. 1 that detects the heat roller temperature.

The fusing temperature that is used in the following sections indicates the target temperature of the heat roller and heat roller temperature is controlled to follow the target temperature. The heat roller temperature, the fusing roller temperature, the fusing roller sensor temperature, and the pressure roller temperature indicate the temperature measured by each sensor.

2.4 *Paper Properties*

Since the objective of this work is to predict the outlet paper temperature in different printing conditions, this experiment involved experiments with 9 types of A3 sized paper with different properties that included basis weight, thickness, smoothness and surface coating as shown in Table II. These properties affect the heat transfer characteristics from the fusing unit to the paper and paper temperature rise.

Basis weight is a unit that represents the weight of paper per square meter. Paper thickness is the thickness of the paper measured with a micrometer.

Smoothness is the degree of surface flatness. Smoothness is measured by pressing the paper against the glass and measuring the time that air passes between them. The unit of smoothness is second. The shorter the passing time is, the more uneven the paper is, because the air is more likely to come out. Therefore, the smaller the number of seconds is, the lower the smoothness is. Generally, the higher the smoothness of the paper, the higher the glossiness.

Table II. Paper properties

Paper type	Basis weight [g/m^2]	Thickness [μm]	Smoothness [s]	Surface coating
A	53	66	82	Non-coated
B	81	94	95	Non-coated
C	156	184	40	Non-coated
D	100	102	788	Coated
E	161	171	731	Coated
F	68	91	47	Non-coated
G	128	149	50	Non-coated
H	133	139	777	Coated
I	127	145	102	Coated

Surface coating is used to obtain a higher finish quality. The coating material is usually the mixture of calcium carbonate and the binder resin.

3. ML ALGORITHM

To predict the outlet paper temperature using the temperature values measured in the experimental set-up shown in Fig. 1, ML algorithm using ANN was developed using TensorFlow [14], Keras [15] and Scikit-learn [16] libraries publicly available for Python programming language.

Generally, prediction modeling methods are divided into a classifier and a regressor. A classifier can predict discrete class label output. A regressor can predict continuous quantity output. In this study, the output value of the ANN is temperature that is a continuous quantity, thus making our ANN a regressor rather than a classifier.

In conventional technologies, thermophysical properties of paper were generally required to predict the outlet paper temperature. However, it is difficult to measure the thermophysical properties of the porous paper, and it is especially difficult to measure the contact thermal resistance between the paper and the fusing nip. In recent years, highly accurate physical models have been developed, but we considered easier machine learning model by using paper properties such as basis weight, thickness and smoothness that are not thermophysical properties. The advantage of this study is that it is easy to handle these properties that can be fed into ML model directly and obtain accurate prediction.

3.1 *Data Preprocessing*

Due to the nature of the experiment, the obtained experimental data needed preprocessing because the raw data measured with the radiation thermometers and contact thermocouple contained a lot of extraneous information for ML. There was a gap between the n-th paper and the $(n+1)$-th paper and there is the period that the sensors measure the temperature of components when the paper

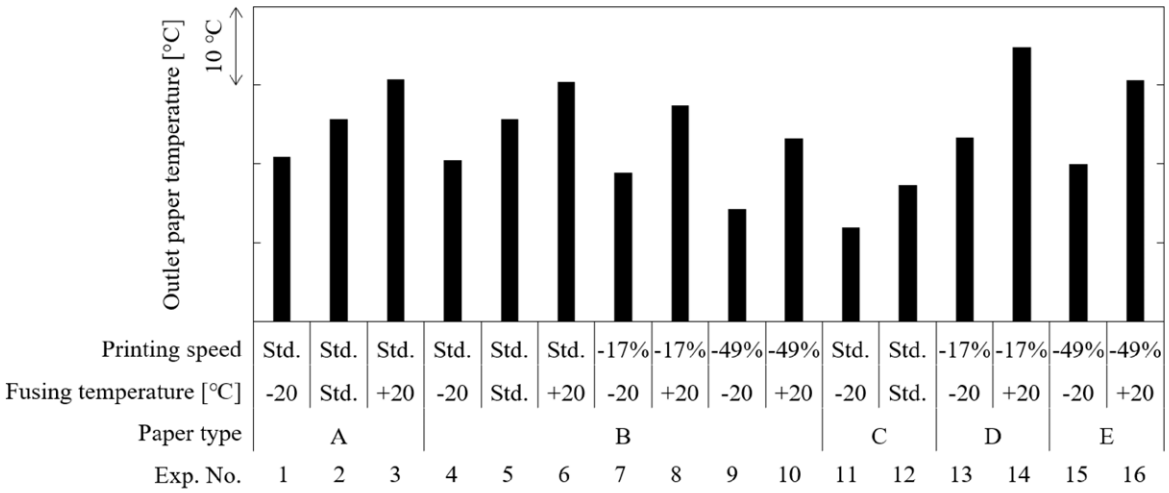

Figure 3. Outlet paper temperatures of training experiments

Table III. ANN configuration

Number of hidden layers	3
Number of neurons of each hidden layer	64, 45, 14
Activation function on hidden layers	ReLU
Activation function on output layer	Linear
Optimizer	Adam

was not passing. There was a large difference of the paper temperature and component temperature between the gap and the paper passing period. Moreover, as there was a slight temperature fluctuation during the period of one sheet passing, the temperature averaging processing was also conducted.

The data was finally scaled between 0 and 1 as it was found during algorithm training that this practice yields better results. After ML was completed, data was restored to the original scale to verify the results on training and validation.

3.2 *ANN Configuration*

JAs is the case in most ML models, ANN configuration plays a crucial role in the performance of the model. Schematic of ANN which was used in this work is shown in Figure 2. ANN configuration is shown in Table III.

ANN of this work comprises of a large number of interconnected neurons. The first layer is the input layer with several inputs. The number of inputs depends on each model. The last layer is output layer with one output. The three middle layers are the hidden layers, and the number of neurons of each hidden layer is 64, 45, 14 respectively. There exists an activation function and a bias on each neuron. The input information is propagated forward through the network.

Adam optimizer [17] was used for updating the weights of neurons. As for the activation function, Rectified Linear Unit (ReLU) was used in the hidden layers and a linear unit was used in the output layer.

Layers of the network were formed by the Dense() function provided by the Keras library [15]. Mean squared error (MSE) was used as the loss function:

$$\mathrm{MSE} = \sum_{i=1}^{n} \frac{(y_i - \hat{y}_i)^2}{n}, \tag{1}$$

where n is the number of data, y_i and $\hat{y}_i$ are the measured and predicted values for the ith data, respectively. Note that MSE was also used when evaluating the performance of the model. The algorithm also used early stopping feature; the training was stopped when no further significant decrease in loss is achieved after each training epoch.

The coefficient of determination R^2 was also used to evaluate the error of the predicted values:

$$R^2 = 1 - \frac{\sum_{i=1}^{n}(y_i - \hat{y}_i)^2}{\sum_{i=1}^{n}(y_i - \overline{y})^2}. \tag{2}$$

3.3 *Experimental Conditions*

There are 20 experimental conditions shown in Table IV. Experiment (Exp.) No. 1 to No. 16 were conducted for the training of the ML model, and Exp. No. 17 to No. 20 were conducted for validation of the ML model.

The conditions of the training experiment were determined as follows. Commonly used paper types were selected, covering the paper properties from 53 g/m^2 to 161 g/m^2 basis weight, from 66 μm to 184 μm thickness, and from 40 s to 788 s smoothness. The fusing temperature of Std., +20°C, −20°C and the printing speed of Standard (Std.), −17%, −49% were the ranges that were used in the actual printing. The printing speed is the speed at which the paper is conveyed, and it is also the peripheral velocity of the fusing roller, heat pipe roller, transfer roller, and photoconductor roller.

Table IV. Experimental conditions

Exp. No.	Paper type	Fusing temperature [°C]	Printing speed [mm/s]	Purpose
1	A	−20	Std.	Training
2	A	Std.	Std.	Training
3	A	+20	Std.	Training
4	B	−20	Std.	Training
5	B	Std.	Std.	Training
6	B	+20	Std.	Training
7	B	−20	−17%	Training
8	B	+20	−17%	Training
9	B	−20	−49%	Training
10	B	+20	−49%	Training
11	C	−20	Std.	Training
12	C	Std.	Std.	Training
13	D	−20	−17%	Training
14	D	+20	−17%	Training
15	E	−20	−49%	Training
16	E	+20	−49%	Training
17	F	+10	Std.	Validation
18	G	−15	Std.	Validation
19	H	+15	−49%	Validation
20	I	−10	−17%	Validation

The verification experiment was conducted at the paper types and the fusing temperatures that were different from those of the training experiment, but the printing speed was selected from the following speeds of Std., −17%, −49%.

The experiment was conducted by printing the test letters on paper while temperature of each paper, and the fusing unit were recorded. One experiment was performed with one type of paper and 500 sheets were printed.

4. RESULTS AND DISCUSSIONS

4.1 *Outlet Paper Temperature of Training Experiment*

Before discussing the results, we considered the difference in outlet paper temperature under each condition obtained in the training experiments. Figure 3 shows the results of the outlet paper temperatures of the training experiments. The ordinate is the 100 sheets average temperatures from the 400th sheet to the 500th sheet when 500 sheets are continuously printed, and those were measured by sensor [4] in Fig. 1. One scale on the ordinate is 10°C.

There was a difference of more than 20°C between the maximum and minimum. It means that the outlet paper temperature depends on paper type, fusing temperature and printing speed. It is easy to understand that different fusing temperatures cause different paper temperature.

When the printing speed is lower, the heating time in the fusing unit is longer, but the period that lowers the paper temperature from the fusing unit to the outlet is also longer, which makes it difficult to predict. For example, although the fusing temperatures of No. 6 and No. 10 were the same, the printing speed of No. 10 was lower than that of No. 6 and a large amount of heat was obtained from the fusing unit. But the period that lowered the paper temperature was longer, then the outlet paper temperature dropped by 7°C.

The type of paper also affected the paper temperature. The fusing temperature and the printing speed of No. 4 and No. 11 were same, but since the paper type was different, the outlet paper temperature difference was 9°C.

Thus, it was confirmed that the paper temperature was significantly influenced by the paper type, the fusing temperature, and the printing speed. In the production printing industry, many types of paper are used for printing, and printing conditions such as fusing temperature and printing speed are numerous. It takes a lot of time to evaluate all conditions and the occurrence of the toner blocking. Therefore, the effectiveness of predicting the paper temperature after the fusing process based on the ML model was shown in the following sections.

4.2 *Outlet Paper Temperature Prediction Model*

In order to predict the outlet paper temperature, the fusing unit temperatures and the paper property shown in Table V were selected as the inputs. The outlet paper temperature was used as the output.

In the first ML model, only the basis weight of the paper was included in the inputs. The basis weight represents mass per area of paper. In general, the basis weight is displayed as part of the product name as an indicator of the paper thickness.

It was tested whether it could be predicted using only the fusing unit temperatures and the paper basis weight which assumed a value that correlates with the heat capacity of the paper.

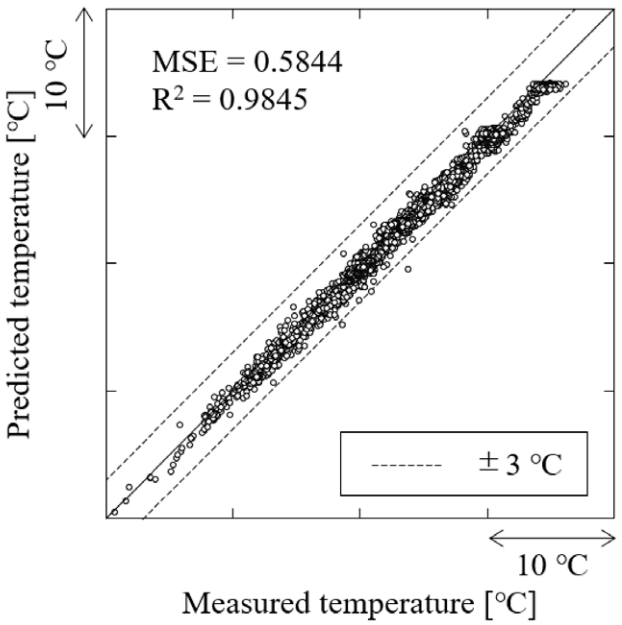

Figure 4. Result of training in outlet paper temperature prediction model.

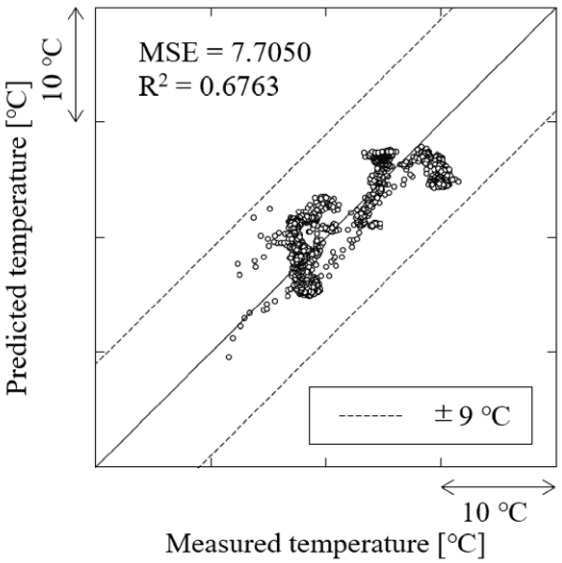

Figure 5. Result of validation in outlet paper temperature prediction model.

Table V. Input and output of outlet paper temperature prediction model

Input	Output
Heat roller temperature	Outlet paper temperature
Fusing roller temperature	
Fusing roller sensor temperature	
Pressure roller temperature	
Printing speed	
Paper basis weight	

Figure 4 shows the result of training in the outlet paper temperature prediction model which was trained with the experiments from No. 1 to No. 16. The predicted temperature was within ±3°C of the measured temperature.

Figure 5 is the result of validation in this model which was validated with the experiments of No. 17 to No. 20. The result was that the difference between the predicted temperature and the measured temperature was within ±9°C and was too large to correctly predict the occurrence of the toner blocking. It is desirable to keep it within ±5°C. MSE and R^2 were not good results either.

Figure 6 is the temperature profile of the verification experiment. The abscissa is the number of printed sheets. In continuous printing of 500 sheets, the measured temperature and the predicted temperature were plotted every 10 sheets. At the beginning of the continuous printing, the paper temperature was low because the temperature of the heat pipe and the paper passing route was also low, then the paper temperature gradually rose and became constant.

Especially in Exp. No. 19, the difference between the predicted temperature and the measured temperature was large.

Table VI. Input and output of outlet paper temperature prediction model with paper thickness added to input

Input	Output
Heat roller temperature	Outlet paper temperature
Fusing roller temperature	
Fusing roller sensor temperature	
Pressure roller temperature	
Printing speed	
Paper basis weight	
Paper thickness	

Table VII. Input and output of outlet paper temperature prediction model with paper thickness and paper smoothness added to input

Input	Output
Heat roller temperature	Outlet paper temperature
Fusing roller temperature	
Fusing roller sensor temperature	
Pressure roller temperature	
Printing speed	
Paper basis weight	
Paper thickness	
Paper smoothness	

4.3 *Outlet Paper Temperature Prediction Model with Paper Thickness Added to Input*

In this section, we examined whether the prediction accuracy could be improved by adding the paper thickness as an input in addition to the paper basis weight as shown in Table VI. Because the paper density assumed a value that correlates with the thermal conductivity of the paper, it can be calculated by using the basis weight and the paper thickness.

Figure 7 shows the result of training in the outlet paper temperature prediction model which was trained with the experiments of No. 1 to No. 16. The predicted temperature was within ±3°C of the measured temperature.

Figure 8 is the result of validation in this model which was validated with the experiments of No. 17 to No. 20. Although MSE and R^2 improved slightly, the difference between the predicted temperature and the measured temperature was still within ±9°C.

Figure 9 is the temperature profile of the verification experiment. Especially in No. 17, the difference between the predicted temperature and the measured temperature was large. The prediction accuracy was improved slightly by adding the paper thickness. However, it did not reach the target value ±5°C.

From those results, although the basis weight and the thickness that were estimated to have a correlation with heat

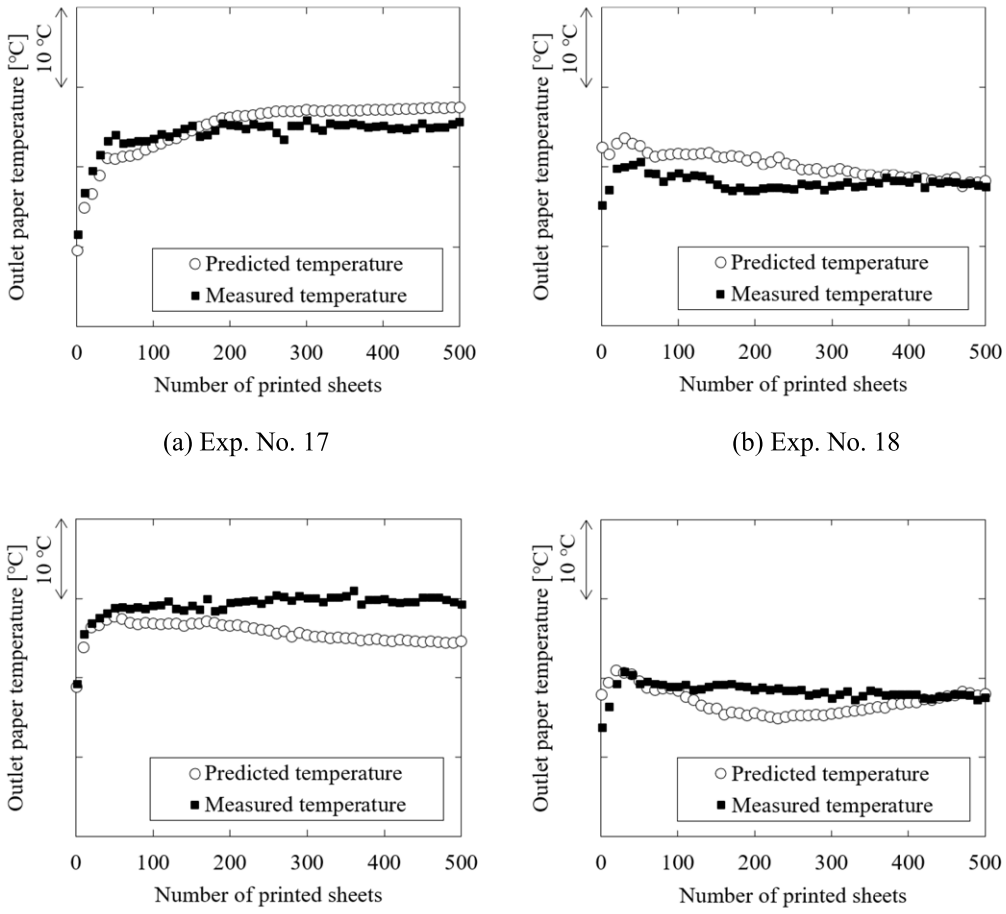

Figure 6. Outlet paper temperature profile of validation experiments in outlet paper temperature prediction model.

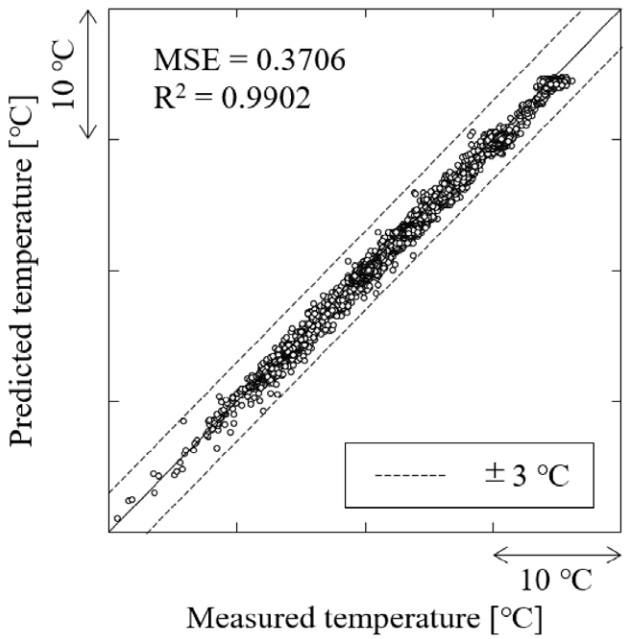

Figure 7. Result of training in outlet paper temperature prediction model with paper thickness added to input.

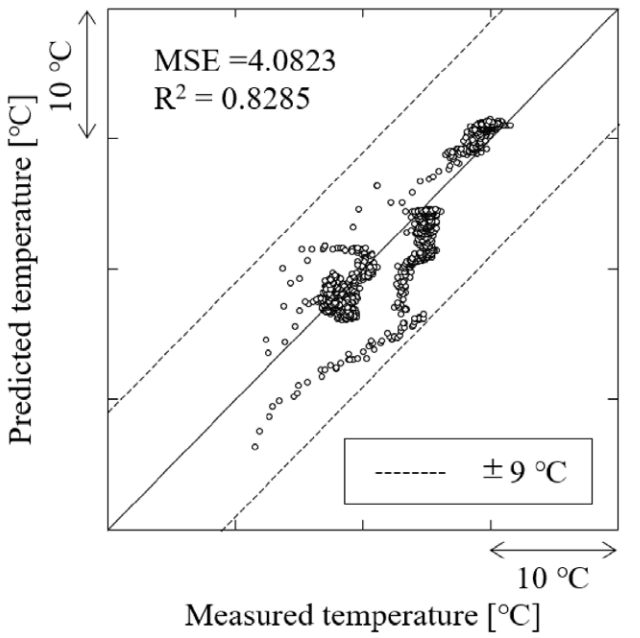

Figure 8. Result of validation in outlet paper temperature prediction model with paper thickness added to input.

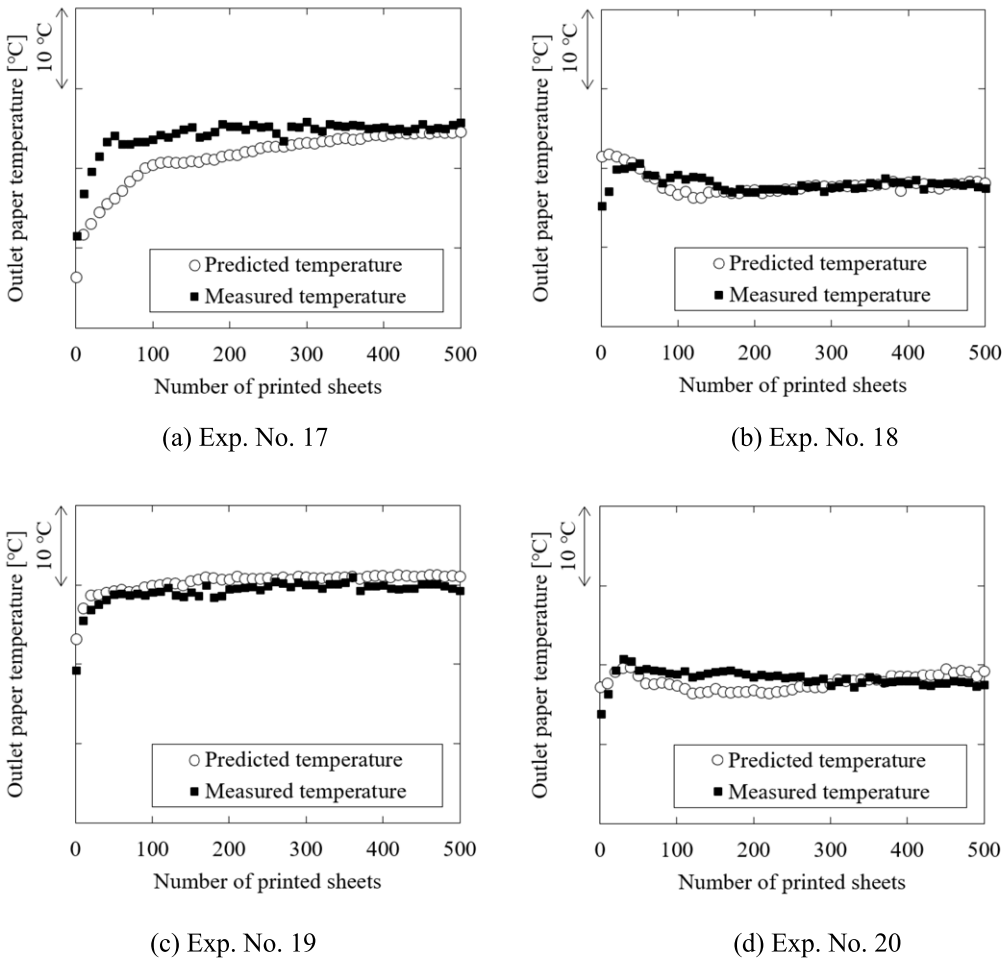

Figure 9. Outlet paper temperature profile of validation experiments in outlet paper temperature prediction model with paper thickness added to input.

capacity and thermal conductivity were included in the input, the target prediction accuracy was not obtained.

4.4 *Outlet Paper Temperature Prediction Model with Paper Thickness and Paper Smoothness Added to Input*

Another possible factor that should be considered is the effect of contact thermal resistance between the paper and the fusing belt, pressure roller, and heat pipe. The surface of paper differs depending on the paper type, and it is presumed that paper with a rough surface has high contact thermal resistance, and paper with a smooth surface has low thermal resistance. Therefore, smoothness that is presumed to correlate with contact thermal resistance was added to the input as shown in Table VII.

Figure 10 shows the result of training in the outlet paper temperature prediction model which was trained with the experiments of No. 1 to No. 16. The predicted temperature was within ±3°C of the measured temperature.

Figure 11 is the result of validation in this model which was validated with the experiments of No. 17 to No. 20. Figure 12 is the temperature profile of the verification experiment. The difference between the predicted temperature and the measured temperature was ±5°C which was within the

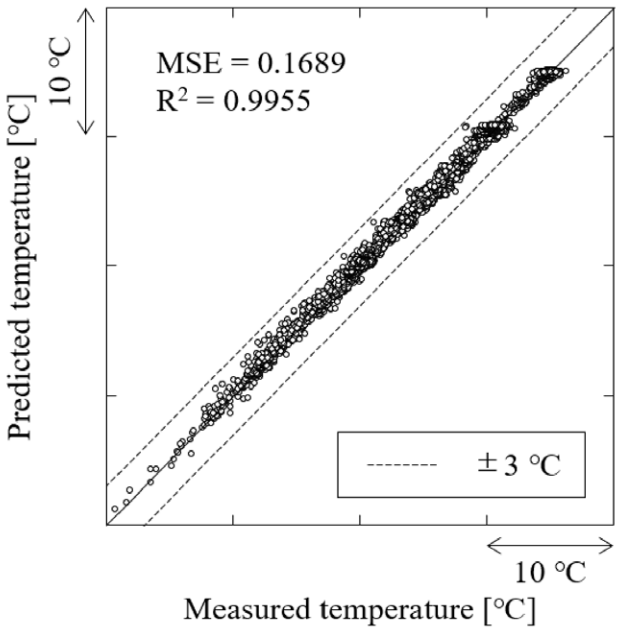

Figure 10. Result of training in outlet paper temperature prediction model with paper thickness and paper smoothness added to input.

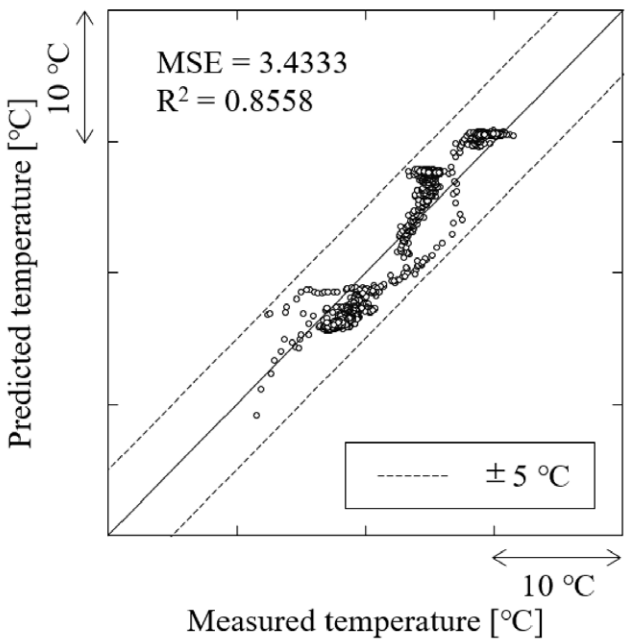

Figure 11. Result of validation in outlet paper temperature prediction model with paper thickness and paper smoothness added to input.

target value. Also, MSE and R^2 were improved compared to the previous models.

It was confirmed that the prediction accuracy was improved by adding the paper smoothness as well as the paper basis weight and the paper thickness to the input. Therefore, it is suggested that there is a correlation with the paper smoothness and contact thermal resistance.

In the previous studies [11, 12], the paper properties were not included in the ANN inputs. It is estimated that the prediction accuracy of the previous studies was probably more than ±9°C if the verification experiment was conducted under different paper type, fusing temperature, and printing speed conditions from the training conditions. This is because the prediction accuracy was ±9°C when only basis weight among the paper properties was input in this study, and the paper properties were not considered in earlier studies. Thus, the ML model including appropriate paper properties could improve the prediction accuracy compared to the previous studies.

5. CONCLUSIONS

In this work, ML algorithm using ANN was applied to paper temperature prediction in the production printing system

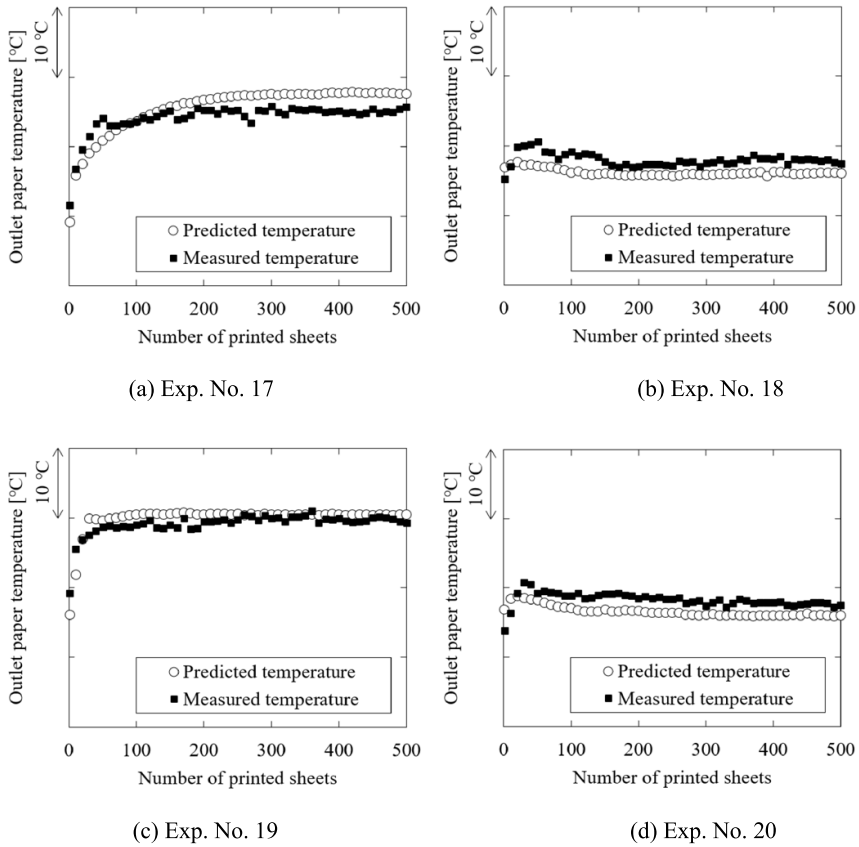

(a) Exp. No. 17

(b) Exp. No. 18

(c) Exp. No. 19

(d) Exp. No. 20

Figure 12. Outlet paper temperature profile of validation experiments in outlet paper temperature prediction model with paper thickness and paper smoothness added to input.

with electro-photography method. It was shown that the outlet paper temperature could be accurately predicted by the simple ML model without relying on a complicated physical model.

By inputting the fusing unit temperatures, printing speed and paper properties of various paper types, we developed the ML model that could predict the outlet paper temperature with high accuracy. Furthermore, it was confirmed that the prediction accuracy was improved by adding the paper smoothness as well as the paper basis weight and the paper thickness to the input. It is suggested that the paper temperature depends not only on the heat capacity and thermal conductivity of the paper, but also on the thermal resistance of the contact between the paper and the fusing unit, heat pipe. This is because the smoothness of the paper represents the contact rate between the paper and the member.

Until now, outlet paper temperature has been evaluated by conducting a lot of experiments, or by developing a complicated physical model. However, ML models enabled accurate and easy temperature prediction. Moreover, although it is usually difficult to handle property values such as the smoothness of paper with a physical model, it was possible to input the value directly. ML algorithm using ANN has the potential to be applied to various thermal designs of the printing system as well as the outlet paper temperature.

REFERENCES

[1] T. Takenaka, M. Iio, K. Matsumoto, T. Asami, T. Sugiyama, A. Yamazaki, S. Akatsu, M. Nakayama, and T. Higa, "New technologies for printed material's advanced value in the production printing market," *Proc. IS&T's NIP27: Twenty-seventh Int'l. Conf. on Digital Printing Technologies and Digital Fabrication 2011* (IS&T, Springfield, VA, 2011), Vol. 27, pp. 537–539.

[2] S. Aoki, H. Iimura, Y. Ogino, K. Nakamura, I. Maeda, N. Sugimoto, and S. Tanaka, "New effect of AC high field on toner transfer," *Proc. IS&T NIP29: Twenty-Ninth Int'l. Conf. on Digital Printing Technologies and Digital Fabrication 2013* (IS&T, Springfield, VA, 2013), Vol. 29, pp. 545–549.

[3] T. Ogawa, "Sheet conveying device, print system, and sheet cooling method," US Patent 8,596,637 (2013).

[4] T. Onishi, K. Kato, M. Kouno, H. Eguchi, Y. Kobaru, and Y. Yoda, "Toner fix simulation in fuser process," J. Imaging Soc. Japan **52**, 515–522 (2013).

[5] H. Al-Rubaiey and P. Oittinen, "Thermal behavior of paper in contact fusing technology," J. Imaging Sci. Technol. **52**, 030507 (2008).

[6] S. A. Lavrykov and B. V. Ramarao, "Thermal properties of copy paper sheets," Dry. Technol. **30**, 297–311 (2012).

[7] D. J. Sanders, D. F. Rutland, and W. K. Istone, "Effect of paper properties on fusing fix," J. Imaging Sci. Technol. **40**, 175–179 (1996).

[8] Y. LeCun, Y. Bengio, and G. Hinton, "Deep learning," Nature **521**, 436–444 (2015).

[9] C. W. Chang and N. T. Dinh, "Classification of machine learning frameworks for data-driven thermal fluid models," Int. J. Therm. Sci. **135**, 559–579 (2019).

[10] M. Oikawa, K. Kanai, and T. Shimada, "AI supported printing on various media for industry printing," OKI Tech. Rev. **230** (2017).

[11] E. Dursunkaya, S. Kawasaki, K. Hemmi, K. Yamazaki, S. Kuramoto, K. Kato, and K. Fushinobu, "Investigation of the effect of paper types on the paper temperature in the electrophotographic process by using machine learning," *Proc. ISTP 30*, ISTP012 (Ha Long, Vietnam, 2019).

[12] S. Kawasaki, K. Yamazaki, K. Hemmi, S. Kuramoto, K. Kato, and K. Fushinobu, "Prediction and control technique of the paper media temperature after fusing in electrophotographic process," *Proc. ASME Inter PACK 2019*, IPACK2019-6396 (Anaheim, USA, 2019).

[13] T. Hase, S. Kawasaki, E. Dursunkaya, T. Ishikura, K. Hemmi, K. Yamazaki, S. Kuramoto, K. Kato, and K. Fushinobu, "Temperature prediction modeling in production printing system by using machine learning," *Proc. ISTP 31*, ISTP091 (Online, 2020).

[14] M. Abadi, A. Agarwal, P. Barham, E. Brevdo, Z. Chen, C. Citro, G. S. Corrado, A. Davis, J. Dean, M. Devin, and S. Ghemawat, "TensorFlow: Large-Scale Machine Learning on Heterogeneous Distributed Systems," arXiv:1603.04467 (2015).

[15] F. Chollet, "Keras," (2015).

[16] F. Pedregosa, G. Varoquaux, A. Gramfort, V. Michel, B. Thirion, O. Grisel, M. Blondel, P. Prettenhofer, R. Weiss, V. Dubourg, and J. Vanderplas, "Scikit-learn: Machine learning in Python," J. Mach. Learn. Res. **12**, 2825–2830 (2011).

[17] D. P. Kingma and J. L. Ba, "Adam: A method for stochastic optimization," *Proc. ICLR 2015* (San Diego, USA, 2015).